

International Conference on High Energy Accelerators, Cambridge, Massachusetts, September 1967 (unpublished).

²D. Keefe *et al.*, Phys. Rev. Lett. **22**, 588 (1969).

³A. W. Trivelpiece *et al.*, Phys. Rev. Lett. **21**, 1436

(1968).

⁴N. C. Christofilos, Phys. Rev. Lett. **22**, 830 (1969).

⁵J. D. Lawson, Phys. Lett. **29A**, 344 (1969).

⁶W. H. Kegel, Plasma Phys. **12**, 105 (1970).

⁷E. Ott and R. Sudan, to be published.

Molecular Vibrations in Liquids: Direct Measurement of the Molecular Dephasing Time; Determination of the Shape of Picosecond Light Pulses

D. von der Linde, A. Laubereau, and W. Kaiser

Physik-Department der Technischen Universität München, München, Germany

(Received 8 March 1971)

Molecular vibrations are coherently excited by an intense light pulse of duration t_p . The rise and decay of the vibrational amplitude is measured with delayed pulses of the same time dependence. The molecular dephasing time τ is obtained when $\tau \gtrsim t_p$, while the shape of the light pulse is found for $\tau \ll t_p$.

In the past the short dephasing time τ of molecular vibrations was inferred from the Raman linewidth of the individual vibration. In this Letter we wish to present a new method for the determination of τ . Molecular vibrations are coherently excited by a first short light pulse and the rise and decay of the vibrational amplitude is measured with a second light pulse properly delayed with respect to the first one. For materials with $\tau \gtrsim t_p$, the material parameter τ can be determined (t_p is the pulse width at half-maximum intensity). On the other hand, the shape of picosecond light pulses is observed using samples with $\tau \ll t_p$. We believe that our investigations represent the first direct measurement of the dephasing time in liquids.¹ In addition we present a novel method for the determination of the shape of picosecond light pulses.

We have made a detailed theoretical study of the development of the vibrational (phonon) field for transient stimulated Raman scattering (SRS) with small conversion of laser into Stokes light. The significance of transient SRS should be stressed here. Our results do not hold for the saturation range² where the phonon distribution $Q(t)$ follows (in part) the pumping pulse (phonon pulses much narrower than the pumping pulse are not generated in this way). The starting differential equations for the vibrational amplitude Q and the Stokes field have been discussed in the literature.^{3,4} In Fig. 1(a) the calculated vibrational amplitude Q/Q_{\max} is plotted as a function t/t_p for three values of t_p/τ : 32, 3.2, and 0.8. The solid curves correspond to incident light pulses of Gaussian time dependence, while

the dashed curve is calculated for a hyperbolic-secant function, a pulse with exponential wings.⁵

It is quite apparent from Fig. 1(a) that the vibrational distribution varies drastically with the parameter t_p/τ . For small values of t_p/τ the exponential decay of the vibrational amplitude is clearly seen from the figure. For large values of t_p/τ the phonon pulse rises and decays very rapidly. It will be shown below that the shape of the laser pulse is measured with this steep phonon pulse.

Experimentally we observed the anti-Stokes component $S(t_D)$ of the scattered probe pulse:

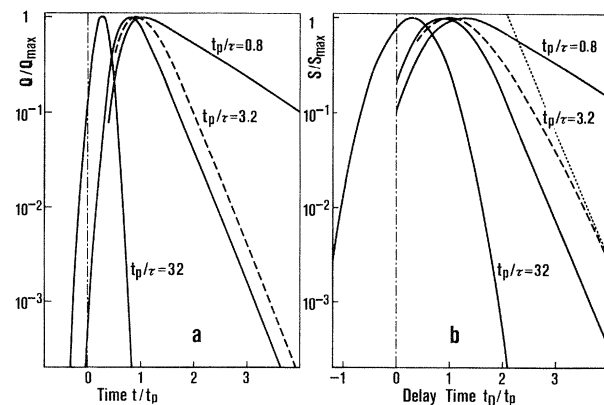


FIG. 1. (a) Calculated vibrational amplitude Q/Q_{\max} versus time t/t_p . t_p is the duration of the exciting and probing light pulse; τ is the dephasing time of the vibration. Solid and dashed curves are calculated for Gaussian- and hyperbolic-secant-shaped light pulses, respectively. (b) Calculated anti-Stokes signal $S(t_D)/S_{\max}$ versus delay time t_D/t_p . For characteristics of the four curves see (a). Dotted line is asymptote with slope τ .

$S(t_D) = \int |E_{AS}|^2 dt$, where the delay time t_D is the time difference between the generating and the probe pulse. We consider the propagation direction of the anti-Stokes field E_{AS} collinear with the propagation direction of the pump pulse since the relevant angles are small in our experimental system (see below). With $t' = t - x/v$, where v is the group velocity, we obtain for the coherent growth of E_{AS}

$$\frac{\partial E_{AS}(x, t')}{\partial x} = \frac{2\pi i \omega_{AS}^2}{c^2 k_{AS}} N \frac{\partial \alpha}{\partial Q} \times e^{ix\Delta k} Q(t' + t_D) E_{L2}(t'), \quad (1)$$

where $\omega_{AS} = \omega_L + \omega_P$ and $k_{AS} = k_L + k_P$ are the frequency of the anti-Stokes field and the corresponding wave vector, respectively. $Q(t' + t_D)$ is the vibrational amplitude generated by the intense pump pulse with electric field $E_{L1}(t' + t_D)$ [see Fig. 1(a)]. N is the number of molecules per cm^3 and $\partial \alpha / \partial Q$ represents the change of polarizability with vibrational amplitude. The phase mismatch is given by $\Delta k = k_{L2} + k_P - k_{AS}$. Integration of Eq. (1) gives the anti-Stokes signal $S(t_D)$ as a function of delay time t_D :

$$S(t_D) = \left(\frac{2\pi \omega_{AS}^2}{c^2 k_{AS}} \right)^2 N^2 \left(\frac{\partial \alpha}{\partial Q} \right)^2 \left(\frac{\sin \frac{1}{2} l \Delta k}{\frac{1}{2} l \Delta k} \right)^2 l^2 \times \int Q^2(t' + t_D) |E_{L2}(t')|^2 dt. \quad (2)$$

The integral in Eq. (2) represents the convolution of the vibrational intensity with the light intensity of the probing pulse. It should be noted that for perfect phase matching, i.e., $\Delta k = 0$, the signal $S(t_D)$ grows with the square of the interaction length l . In Fig. 1(b), calculated values of $S(t_D)/S_{\text{max}}(t_D)$ are plotted versus delay time t_D/t_p for the same phonon fields discussed in Fig. 1(a).

The following points should be noted. For small values of t_p/τ and large delays t_D/t_p the anti-Stokes signal decays exponentially with τ , allowing the direct determination of the dephasing time τ . For intermediate values of $t_p/\tau \approx 3$ the shape of the $S(t_D)$ curve depends strongly on the form of the probe pulse. Rapidly decreasing Gaussian probe pulses give a $S(t_D)$ curve which decreases exponentially with τ starting approximately a factor of 5 below the maximum. On the other hand, probe pulses with larger wings give substantially different $S(t_D)$ curves. As an example, the change of $S(t_D)$ for an exponentially decaying probe pulse (hyperbolic secant) is depicted in Fig. 1(b) (dashed line). In this case the

curvature of the $S(t_D)$ curve changes continuously for a considerable range of values of t_D/t_p ; the exponential slope, which allows the determination of τ (dotted line), begins approximately two orders of 10 below the maximum. Finally, the situation for large values of t_p/τ should be discussed. It is clearly seen from Fig. 1(b) that the $S(t_D)$ curve represents to a good approximation the shape of the Gaussian-probe pulse. For instance the calculated $S(t_D)$ curve deviates from the Gaussian function by only several percent for $t_p/\tau = 32$. Similarly, probe pulses with other time dependence are readily analyzed by measuring the anti-Stokes signal $S(t_D)$ as a function of delay time t_D with large values of t_p/τ (see below). It is important to emphasize the changing properties of the $S(t_D)$ curves: The position of the maximum is located near $t_D/t_p = 1$ for $t_p/\tau \approx 3$ and shifts closer to the ordinate for larger values of t_p/τ . The form of the wings varies strongly with the parameter t_p/τ and with the shape of the probe pulse.

In Fig. 2 our experimental system is depicted schematically. It consists of a mode-locked Nd-glass laser which is followed by an optical shutter⁶ to cut a single picosecond pulse out of the pulse train. A careful analysis of this pulse suggests good mode locking of our system.⁷ Possible frequency modulation (chirp) is small in our pulses. Measurements of the two-photon fluorescence (TPF)⁸ gave contrast ratios very close to

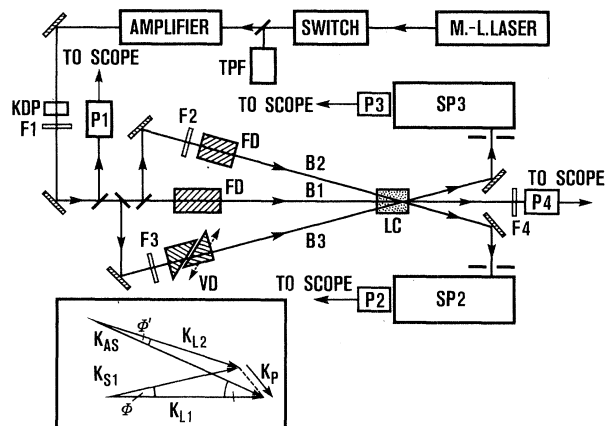


FIG. 2. Schematic of experimental system. Three light beams, $B1$, $B2$, and $B3$, interact in the sample, LC ; glass pieces make the fixed delays, FD , and the variable delay, VD ; filter F ; spectrometer SP ; photo-detector P ; two-photon fluorescence system TPF . Inset: Schematic of noncollinear phase-matched probe anti-Stokes scattering. k_{L1} and k_{L2} are the directions of the intense generating pulse and probe pulse, respectively.

3 (no suppicosecond structure). The single pulse passes an optical amplifier, a potassium dihydrogen phosphate crystal for conversion to the second-harmonic frequency (18.868 cm^{-1} , corresponding to a wavelength of $0.53 \text{ }\mu\text{m}$), and finally enters the measuring cell. The powerful incident pulse (index 1) traverses the medium generating molecular vibrations and Stokes-shifted light. The laser and first Stokes pulse are measured with the fast photocells $P1$ and $P4$; they allow an estimate of the conversion efficiency. It was ascertained in our investigations that the conversion efficiency was small (several percent) in order to stay within the range of validity of our theoretical investigations. Two beam splitters provide two light pulses (indices 2 and 3) of small intensity, approximately 10^{-3} of the pumping pulse. One pulse (index 3) with variable time delay t_D served as probe pulse for the vibrational field in the medium, while a second probe pulse (index 2) with fixed time delay was used as a reference signal to improve the accuracy of our measurements. The optical delays were carefully determined taking the group velocities of the glass specimen into account. The accuracy of the t_D scale is better than 5%, while the absolute position of the origin is known to approximately 2 psec. Both probe pulses are coherently scattered by the molecular vibrations.⁹ In our system the anti-Stokes signals were observed with the help of two spectrometers. The insert in Fig. 2 indicates schematically the scattering process. The laser (k_{L1}) and first Stokes wave (k_{S1}) generate the phonon (k_P); the probe beam (k_{L2}) interacts with the same phonon (k_P) to give the observed anti-Stokes wave (k_{AS}). In reality the various angles are small. We have adjusted our system for close phase matching, with the phonon wave vector k_P collinear with k_{L2} and k_{AS} , i.e., $\Phi' = 0$. Phase matching is facilitated for two reasons: (a) On account of our beam geometry, beam diameter/cell length $\approx 2 \times 10^{-2}$, the vibrational amplitude is still large for $\theta \approx 10^{-1}$. (b) The small interaction length l of the probe and pump beams makes $l\Delta k < \pi$, even for phonon wave vectors k_P close to the forward direction (k_{L1}).

In Fig. 3 we present our experimental data. The anti-Stokes signal $S(t_D)$ of the probe beam (3) is plotted versus the delay time t_D for carbon tetrachloride ($\omega_p/c = 459 \text{ cm}^{-1}$) and ethyl alcohol ($\omega_p/c = 2928 \text{ cm}^{-1}$). The experimental points are average values of five to ten individual measurements. The signal-to-background ratio was

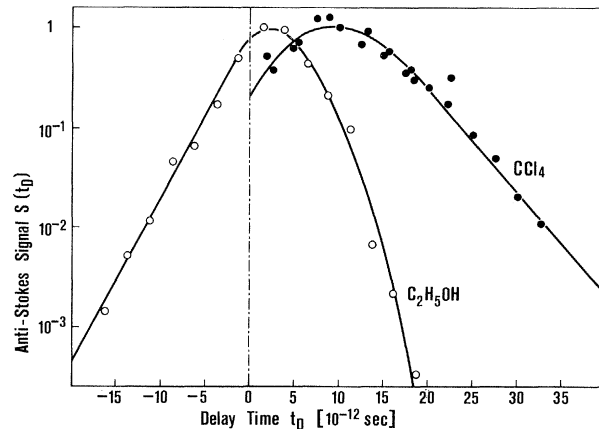


FIG. 3. Measured anti-Stokes signal $S(t_D)/S_{\max}$ versus delay time t_D for ethyl alcohol and carbon tetrachloride. The curve drawn through the experimental points of CCl_4 is calculated.

larger than 200 and 3000 for CCl_4 and $\text{C}_2\text{H}_5\text{OH}$, respectively. First we wish to discuss our results with ethyl alcohol. Spontaneous Raman data of the 2928-cm^{-1} vibration indicate a line-width $\Delta\omega/c \approx 20 \text{ cm}^{-1}$ which suggests a relaxation time $\tau = 0.26 \text{ psec}$. On the other hand, the TPF technique gives a duration of our light pulses of $t_p = 8.3 \text{ psec}$. From these data we estimate $t_p/\tau \approx 32$ for ethyl alcohol. It has been pointed out above [see Eq. (2)] that for large values of t_p/τ , the $S(t_D)$ curve gives direct information on the shape of the probe pulse.¹⁰ In fact, Fig. 3 gives a direct picture of our light pulse. We can infer from Fig. 3 that the probing pulse is asymmetric, rising sharply close to a Gaussian function and decaying exponentially.¹¹ The experiment gives $t_p = 8 \pm 1 \text{ psec}$. The observed asymmetry of the light pulse is expected on account of the finite relaxation time of the bleachable dye in our passively mode-locked laser.¹² Figure 3 shows clearly that our experimental data are—over three orders of magnitude—well accounted for by a Gaussian and an exponential function.

We now turn to the discussion of our measurements in CCl_4 . Our data of Fig. 3 exhibit a shift of the maximum to a value of $t_D \approx t_p$ which is expected for the more transient situation of CCl_4 and a distinct exponential decay for large values of t_D . From the exponential tail of the $S(t_D)$ curve we find the dephasing time of CCl_4 : $\tau = 4.0 \pm 0.5 \text{ psec}$. Knowing the shape of the probe pulse, we are now in the position to compare our experimental data quantitatively with the calculations outlined above. In Fig. 3 the theoretical curve calculated for the pulse shape found

in the experiment with ethyl alcohol ($t_p/\tau = 2.0$) is drawn through the experimental points. The calculated curve fits our data quite well at $t_D = 0$, at the position of the maximum, and also for larger values of t_D . The comparison with theory confirms the dephasing time of $\tau = 4$ psec. It is interesting to compare this value of τ with measurements of the spontaneous Raman line-width. Earlier data suggested a value of $\Delta\omega/c \cong 10 \text{ cm}^{-1}$. More recently the isotope structure of the Raman emission in CCl_4 has been resolved and $\Delta\omega/c \cong 1.5 \text{ cm}^{-1}$ was reported for the most prominent Raman line.¹³ Quite obviously our experimental dephasing time of $\tau = 4.0 \pm 0.5$ psec corresponds to the width of the individual isotope components of the Raman line.

Finally, we wish to emphasize once more the importance of knowing the shape (the wings) of the laser pulse. The determination of a dephasing time of $\tau = 4$ psec with a probe pulse width of $t_p = 8$ psec requires rapidly rising (Gaussian) pulses. Calculations show, for example, that with a Lorentzian pulse of the same duration ($t_p = 8$ psec), only τ values larger than ≈ 80 psec can be measured.

Investigations of the type discussed here are readily extended to other media, to compressed gases and especially to solids where TO phonons (e.g., in diamond¹⁴) and internal vibrations (e.g.,⁹ in CaCO_3) have been excited by stimulated Raman scattering. Using two incident pumping beams with the proper frequency difference, it will be possible to excite molecular and lattice vibrations with smaller gain factors.

The authors wish to acknowledge valuable dis-

cussions with Dr. M. Maier.

¹Our investigations should be contrasted to the measurements of the lifetime τ' of the excited vibrational state. In this case spontaneous Raman scattering of excited H_2 molecules was observed by F. DeMartini and J. Ducuing, *Phys. Rev. Lett.* **17**, 117 (1966). The relaxation times τ' and τ correspond in the Bloch equations to T_1 and T_2 , respectively. Very recently, internal vibrations in CaCO_3 were investigated "by measuring the intensity of spontaneously Raman-scattered light" of a picosecond probe pulse [R. E. Alfano, *Bull. Amer. Phys. Soc.* **15**, 1324 (1970)].

²D. von der Linde, M. Maier, and W. Kaiser, *Phys. Rev.* **178**, 11 (1969).

³M. Maier, W. Kaiser, and J. A. Giordmaine, *Phys. Rev.* **177**, 580 (1969).

⁴S. A. Akhmonov, *Mater. Res. Bull.* **4**, 455 (1969); R. L. Carman, F. Shimizu, C. S. Wang, and N. Bloembergen, *Phys. Rev. A* **2**, 60 (1970).

⁵Gaussian function: $I_L(t)/I_L(0) = \exp\{-[2(\ln 2)^{1/2}t/t_p]^2\}$; hyperbolic secant function: $I_L(t)/I_L(0) = \text{sech}[2 \times \ln(2 + \sqrt{3})t/t_p]$.

⁶D. von der Linde, O. Bernecker, and A. Laubereau, *Opt. Commun.* **2**, 215 (1970).

⁷D. von der Linde, O. Bernecker, and W. Kaiser, *Opt. Commun.* **2**, 149 (1970).

⁸J. A. Giordmaine, P. M. Rentzepis, S. L. Shapiro, and K. W. Wecht, *Appl. Phys. Lett.* **11**, 216 (1967).

⁹J. A. Giordmaine and W. Kaiser, *Phys. Rev.* **144**, 676 (1966).

¹⁰A detailed account will be published elsewhere.

¹¹Note: For positive delays the rise (front) of the probe pulse interacts with the narrow phonon field.

¹²V. S. Letokhov, *Zh. Eksp. Teor. Fiz.* **55**, 1077 (1968) [*Sov. Phys. JETP* **28**, 562 (1969)].

¹³J. Brandmüller, K. Burchard, H. Hacker, and H. W. Schrötter, *Z. Angew. Phys.* **22**, 177 (1967).

¹⁴A. K. McQuillan, W. R. L. Clements, and B. P. Stoicheff, *Phys. Rev. A* **1**, 628 (1970).

Lattice Gas with Short-Range Pair Interactions and a Singular Coexistence-Curve Diameter*

N. D. Mermin†

Istituto di Fisica "G. Marconi," Università di Roma, Rome, Italy

(Received 18 February 1971)

A simple lattice gas, of the familiar kind with only short-range pair interactions, is proved to have a coexistence curve whose diameter is singular at the critical point. Particle-hole symmetry is violated only because the range of interaction energies a molecule can experience depends on which of two nonequivalent sets its lattice site belongs to.

Theoretical analysis has cast doubt on the validity of the law of the rectilinear diameter, which asserts that $d\rho_d(T)/dT$ is asymptotically constant at the liquid-vapor critical point $\{\rho_d(T) = \frac{1}{2}[\rho_V(T) + \rho_L(T)]\}$. Three models have now been described with diameters reflecting the constant-

volume specific-heat singularity¹⁻³:

$$d\rho_d(T)/dT \sim \text{const} \times c_v, \quad T \rightarrow T_c. \quad (1)$$

One can argue that each of these models is atypical. That of Hemmer and Stell¹ is one dimensional, requires forces of infinite range, and